Reactivity of Mesoporous Carbon Against Water – an In-Situ XPS Study

Authors: Sylvia Reiche[a], Raoul Blume[b], Xiao Chen Zhao[a], Dangsheng Su[a], Edward Kunkes[a], Malte Behrens[a], Robert Schlögl[a]*

[a] Fritz Haber Institute of the Max Planck Society, Department of Inorganic Chemistry, Faradayweg 4-6, 14195 Berlin, Germany

[b] Helmholtz-Zentrum Berlin für Materialien und Energie, Albert-Einstein-Str. 15, 12489 Berlin, Germany

Abstract

Functionalized mesoporous carbon catalysts can be used in the acid catalyzed dehydration of fructose to 5-hydroxymethyl furfural (HMF). However, strong deactivation can be observed after preconditioning of the material in the reaction solvent 2-butanol. Surface changes caused by the pretreatment have been studied by XPS. The comparison of the pristine sample and the pretreated carbon sample showed similar distribution of oxygen functional groups by ex-situ XPS, as well as similar behavior during heating in vacuum. However, the addition of water (0.1 mbar vapor pressure) and subsequent heating to 130°C exhibited prominent differences in the evolution of the O1s, as well as for the C1s spectra of the two samples. Changes in the surface termination and hydrophobicity of the materials are discussed under the aspect of possible reactions of surface functional groups with the alcoholic solvent and water.

*Corresponding author. Tel: +49 3084 134404. Fax: +49 3084 134401. E-mail address: acsek@fhi-berlin.mpg.de

1. Introduction

Mesoporous carbon materials from resorcinol-formaldehyde aerogels have attracted enormous attention due to their advantageous properties and multiple potential applications, ranging from electrode materials in supercapacitors and fuel cells, over filters, down to catalytic supports or catalysts [1-4]. Several studies on material texture and pore structure are reported [5, 6]. However, the detailed chemical surface structure is still under investigation. Surface analytical methods, such as X-ray photoelectron spectroscopy (XPS), have been used to quantify the total surface oxygen content of the mesoporous carbon [6]. However, the identification of the nature and the abundance of specific oxygen functional groups are still not understood. Based on the structural elements of the monomers and the polymerization mechanism suggested by Pekala [7], there is a general agreement on the functional groups of the aerogel [7-8]. Isotope exchange experiments combined with 13C-NMR confirmed the abundance of methylene bridges and ether bridges in the polymer [8]. The elucidation of the surface functional groups of the carbonized material was the intention of the present study. The focus was on an improved understanding of changes of surface functional groups by contact to aqueous reaction media as used in multiple applications.

We applied oxidized mesoporous carbon materials as catalysts in the dehydration of fructose to 5-hydroxymethyl furfural (HMF). The carbon-based catalyst showed significant deactivation from exposure to the solvent 2-butanol. The better understanding of this deactivation procedure is necessary for the development of stable heterogeneous catalysts. For this reason, we investigated dynamic changes in electronic surface structures and in the distribution of oxygen functional groups by in-situ XPS, i. e. under vapor exposure and heat treatments to reaction temperature of typically dehydration reactions of fructose (130°C). The vapor pressure of 0.1 mbar was applied in order to study the reactivity of the functionalized carbon surface towards water. Furthermore,

the addition of vapor simulates the water evolution of 3 H_2O molecules per synthesized HMF molecule during the dehydration reaction of fructose.

2. Experimental

2.1 Material synthesis and preliminary characterization

For the synthesis of MC_0, 5.5 g of resorcinol and 5.0 g of formaldehyde solution (37 wt%) undergo an acid catalyzed polymerization in 50 ml of a water-ethanol-mixture (1:1 by weight). The obtained polymer is carbonized in N_2 atmosphere at 350°C and 600°C for 2h, respectively. The detailed procedure of OMC synthesis is described elsewhere [4]. After the carbonization, the mesoporous carbon is oxidized by H_2O_2 in a mixture of methanol and 2 M HCl (1:1, V:V) to obtain MC_1. The preconditioned material MC_2 was synthesized of MC_1 by stirring in 2-butanol at 130°C for 15h. For the 2-butanol treatment a 200-ml Parr autoclave (Series 4560) was used.

All materials are mesoporous carbons (Table 1). The BET surface areas were determined by measuring the adsorption-desorption-isotherms with a Quantachrome Autosorb automatic BET-sorptometer at -196°C with nitrogen as analysis gas. For data evaluation the Quantachrome software Autosorb1 (version 1.54) was used. A full list of BET isotherms and plots for the BJH pore size distribution can be found in the supplementary information. The number of acid functional groups was determined by titration using an automatic titrator (Mettler Toledo). For each measurement, 100 mg catalyst were dispersed in 10^{-3} mol KCl-solution and stirred over night. Following the carbon dispersion was titrated under Ar atmosphere, using a 0.1 M NaOH solution. TG-MS was performed in a thermo-microbalance by Netzsch (STA 449 C). Mass loss and ion currents of released gases were recorded while heating 30 mg MC_1 at 5 K/min in Ar (70 ml/min).

Table 1: Summary of material basis including BET areas and titration results

Sample	Material description	BET [m²/g]	Acid sites [mmol/g]
MC_0	ordered mesoporous carbon	789	n. d.[b]
MC_1	mesoporous carbon, functionalized by H_2O_2 at pH = 1	596	0.24[a]
MC_2	mesoporous carbon, MC_1 after preconditioning in 2-butanol at 130°C for 15 h	604	n. d.[b]

[a] density of acid sites determined by titration of the material (100 mg in 50 ml KCl 0.001 M) with 0.01 M NaOH.

[b] n. d. – not determined

2.2 Instrumental

In-Situ XPS experiments were performed at the synchrotron radiation source BESSY II of the Helmholtz Zentrum Berlin (HZB). The in-situ chamber was designed by the Fritz Haber Institute of the Max Planck Society [10-13]. A schematic sketch of the set up is depicted in Figure 1. The high-pressure reaction cell is separated from the X-ray source by an X-ray transparent window. The emitted electrons attain the hemispherical electron analyzer through three differentially pumped apertures.

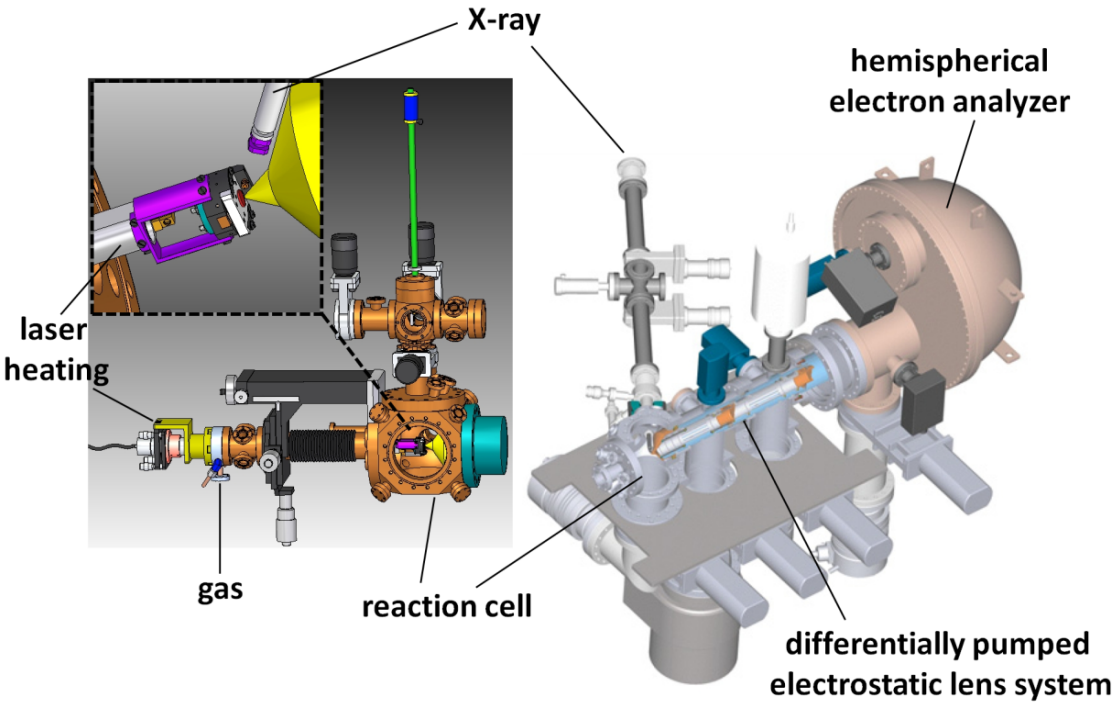

Figure 1: Schematic drawing of the high pressure XPS system at BESSY II [10-13].

During in-situ XPS analysis of MC_1 and MC_2, the samples were heated stepwise to 130°C in vacuum and subsequently exposed to water at 0.1 mbar. In a second experiment, the samples were heated from RT to 130°C in water atmosphere (0.1 mbar). Spectra of the C1s and O1s regions as well as their respective Fermi edges were recorded with an electron kinetic energy of ~150eV. Furthermore, chlorine impurities were detected. Hence, the Cl2p region was recorded additionally. The detailed comparison of the materials concerning there chlorine impurity level can be found in the supporting information.

All spectra are normalized to the background on the high binding energy side for better comparison of the peak shape of the main component. The spectra were fitted with a set of peaks derived from a differential spectra survey of a large number of functionalized and unfunctionalized carbon samples.[2]

[2] Blume R. unpublished work. Berlin 2011

3. Results and Discussion

3.1 Differences in original carbon samples

In order to investigate changes in the electronic surface structure and oxygen functional groups after the pretreatment in 2-butanol, we have chosen two representative samples for insitu XPS experiments. The first mesoporous carbon sample was functionalized in hydrogen peroxide at pH 1 and corresponds to an active catalyst in the dehydration of fructose into HMF (MC_1). Secondly, a sample MC_2 was obtained by a pretreatment of MC_1 in reaction solvent at reaction temperature, i. e. in 2-butanol at 130°C. In addition, a reference sample MC_0 was examined.

In a first step the samples MC_1 and MC_2 were investigated ex-situ and compared to the reference sample MC_0 that represents the mesoporous carbon before any oxidation treatment. According to Blume[3], the O1s spectra were fitted by 6 different components of the peak positions 530.5 eV, 531.2 eV, 531.9 eV, 532.7 eV, 533.5 eV and 534.2 eV (Table 2). An additional feature for the measurements under water vapor was detected at 535 eV and corresponds to the water gas phase peak [14].

The assignments of specific features in the O1s peak are intensively and partially controversially debated in the literature (Table 2). It is generally agreed to the discrimination of minimum two different oxygen species, the double bonded oxygen at lower binding energies (~531 eV) and the single bonded oxygen at higher binding energies (~533 eV) [15]. Additionally, a third species at higher binding energies is commonly considered in the fit, assigned to adsorbed water or oxygen [14, 16-20]. Clark et al. performed more detailed studies in the systematic comparison of well defined polymers and suggested the discrimination of four different oxygen species: double-bonded oxygen in esters, carbonates and acids (~532.8–532.9 eV), oxygen in ketons, ethers and

[3] Blume R. unpublished work. Berlin 2011

alcohols (~533.6–533.7 eV), single-bonded oxygen in acids and esters (~534.3 eV) and single-bonded oxygen in carbonates (~535.0–535.2 eV) [21-22]. The high resolution of modern XPS instruments, the use of synchrotron radiation sources, and the consideration of the thermostability of different oxygen functional groups lead to verification of the Clark model [23-25] and further differentiation of the O1s peak [26-29].

Table 2: O1s peak assignment according to the literature

<table>
<tr><th>No.</th><th>Peak position [eV]</th><th>Oxygen functional group</th><th colspan="2">Supporting References</th></tr>
<tr><td>I</td><td>530.5</td><td>C=O in quinones</td><td colspan="2" rowspan="2">[14, 16-20, 25, 26]</td></tr>
<tr><td>II</td><td>531.2</td><td>C=O in ketones, aldehydes</td></tr>
<tr><td>III</td><td>531.9</td><td>C-O-C in aromates (furan), or keto-enol tautomers</td><td rowspan="3">[14, 16-20]</td><td></td></tr>
<tr><td rowspan="2">IV</td><td rowspan="2">532.7</td><td>OH in phenol or aliphatic alcohols</td><td>[26]</td></tr>
<tr><td>chemisorbed H2O</td><td></td></tr>
<tr><td>V</td><td>533.5</td><td>C-O-C in ethers, esters, anhydride</td><td>[26, 28]</td></tr>
<tr><td rowspan="2">VI</td><td rowspan="2">534.2</td><td>C-OH in carboxylic acid</td><td colspan="2">[17, 20, 26, 27, 33]</td></tr>
<tr><td>chemisorbed H2O</td><td rowspan="2">[14, 16-20]</td><td>[28]</td></tr>
<tr><td>VII</td><td>535</td><td>gas phase H2O</td><td>[14]</td></tr>
</table>

For the present work we also tried to involve considerations on structural elements that are predetermined by the synthesis procedure. Based on the polymeric precursor of the mesoporous carbon a broad variety of oxygen functional groups is possible for the carbon samples. Most likely the material still contains phenolic and aliphatic OH-groups, as well as ether groups after the carbonization procedure. Due to possible condensation reactions at the applied temperatures (600°C for 2 h during carbonization), lactones, furans or quinones are further possible structural

elements. During the oxidation in hydrogen peroxide an increase in carbonyl and carboxyl groups is expected, as well as further hydroxyl functional groups through the oxidation of double bonds. Comprising the knowledge of the building blocks, the synthesis procedure and experiences reported in the literature [29-31], a schematic carbon structure can be proposed for the materials (Figure 2). In the following, this structural idea will be compared to the result of the XPS experiments.

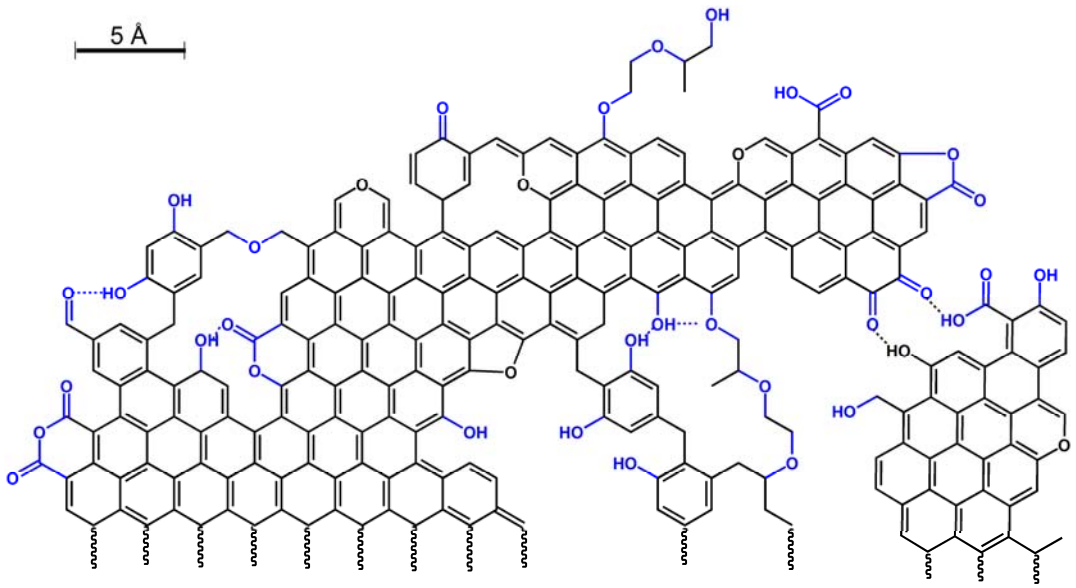

Figure 2: Scheme of possible carbon structure for the samples investigated in consideration of the structural elements of the polymeric precursor and ideas reported in the literature [29-31]. In blue: functional groups that can interact with water molecules under the formation of hydrogen bonds or in hydrolysis reactions.

Ex-situ measurements of MC1 and MC_2 show O1s spectra of similar line shape for both samples (Figure 3). There is only a small difference in the total oxygen content of about 1%. The small intensity difference is equally distributed between the species II-V. However, the

component VI at 534.2 eV, which can be assigned to carboxylic acid functional groups [25, 26] or chemisorbed water [14, 16-20] according to the literature, is abundant in slightly higher proportion in sample MC_1 in comparison to the sample MC_2 after the butanol treatment. Either assignment could support the idea of possible surface changes of MC_1 during the treatment in alcoholic solvents. In the case of the assignment to carboxylic acid functional groups, the lower content for MC_2 could be explained by possible esterification reactions in the alcoholic solvent. If assigned to adsorbed water, the higher content of the species at 534.2 eV points to a higher hydrophilicity for MC_1 which can be seen as indirect evidence for surface modifications by 2-butanol in the case of MC_2.

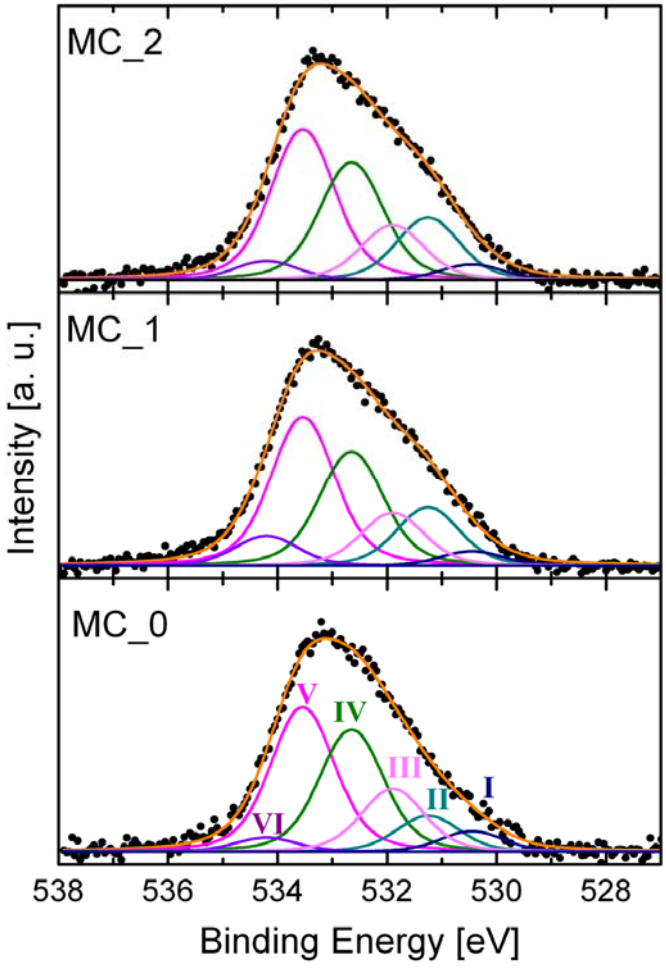

Figure 3: O1s fits of MC_0, MC_1 and MC_2 of ex-situ XPS measurements.

The total oxygen content of the reference sample MC_0 is approximately half the oxygen content of MC_1 and MC_2. In contrast to the oxidized samples, the O1s spectrum of MC_0 differs in line shape due to the lower influence of features at lower binding energies. After the oxidation, the carbonyl species at 531.2 eV contributes stronger to the overall line shape for the samples MC_1 and MC_2.

Similar to the O1s spectra, the C1s peaks (Figure 4) were fitted by a set of fitting parameters derived from a differential spectra survey of a large number of functionalized and unfunctionalized carbon samples[4]. Within the C1s peak, eight features at the positions 284.4 eV, 284.7 eV, 285.2 eV, 285.9 eV, 286.6 eV, 287.9 eV, 288.5 eV and 289.1 eV were discriminated (Table 3). However, due to the dominant influence of the asymmetry of the sp^2 carbon peak (I_{max} = 284.4 eV) up to high binding energies, the quantification of the oxygen species in the C1s is rather difficult. Small errors in the subtraction of the graphitic peak can lead to large errors in the evaluation of the functional groups, in particular due to their minor contribution [32].

[4] Blume R. unpublished work. Berlin 2011

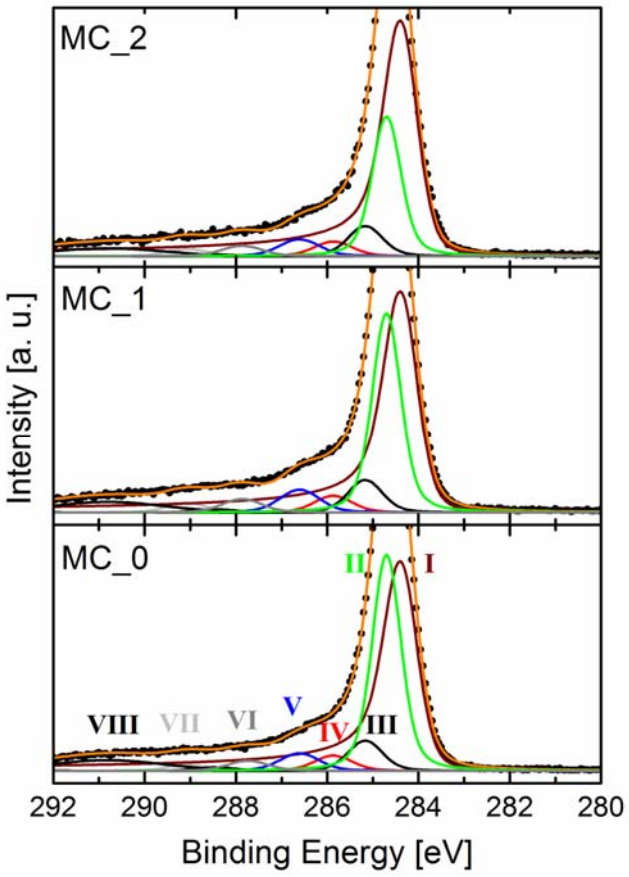

Figure 4: C1s fits of MC_0, MC_1 and MC_2 of ex-situ XPS measurements.

Table 3: C1s peak assignment according to literature

No.	Peak position [eV]	Carbon functional group	Supporting References	
I	284.4	C=C, sp^2 carbon	[17, 20, 26, 27, 33]	
II	284.7	C-C, sp^3 carbon	[17, 20, 26, 27, 33]	
III	285.2	aliphatic C-H, C-O in alcohols, phenols, ethers	[17, 20, 26, 27, 33]	
IV	285.9	C=C-O in keto-enolic equilibria or furans	[13, 15]	[14, 23]
V	286.6	C=O		[14, 23]
VI	287.9	COOH, COOR in carboxylic acids or esters	[17, 20, 26, 27, 33]	
VII	288.5	carbonate	[17], [34]	
VIII	289.1	π-π* satellite	[34]	

Comparing the fits of the C1s spectra for the three samples (Peak I, Figure 4) a clear difference in the proportion of graphitic carbon (= sp^2-carbon) to amorphous carbon and/or unsaturated bonds (= sp^3-carbon) can be found. The higher percentage of graphitic surface carbon for MC_2 can be explained by partial removal of amorphous carbon species during the pretreatment in 2-butanol, since functionalized unstructured carbon is easier to be dispersed in the alcoholic solvent. As consequence of the possible esterification of carboxylic acid functional groups, the abundance of structure determining hydrogen bonds decreases. Hence, the predominant influence of π-π-stacking interactions can result in more densely packed regimes of graphitic carbon. For further structural insights, complementary HR-TEM investigations are required.

The peaks III-VII correspond to the oxygen functional groups. Based on the quantification of the same, lower oxygen content was determined for the reference sample MC_0 which is in agreement to the findings of the O1s spectra evaluation.

3.2 Differences during heating in vacuum

The O1s spectra show similar behavior for MC_1 and MC_2 while heating the materials in vacuum to 130°C. For both samples, a decrease in the total oxygen content of about a seventh part for MC_1 and about one-fifth for MC_2 can be determined (Table 4). Even the water exposure at 130°C does not change the trend of the gradual decrease of most oxygen components. The major change in the oxygen species distribution is observed for the feature at 532.7 eV. Due to the mild temperatures applied, the loss of adsorbed water species from the highly porous materials (compare BET surface areas in Table 1) seems to be another plausible conclusion. TG-MS experiments were performed in order to check for carbon decomposition reactions under CO_2 evolution at the temperatures applied in the in-situ experiments. It could be confirmed that water

is the only released species within the investigated temperature range (Figure 5). The most pronounced intensity after the heating experiments corresponds to an oxygen species at 533.5 eV. As described before this feature can be assigned to ether-like oxygen functional groups which were expected to be stable in the applied temperature treatment.

Table 4: Quantification of oxygen species of MC_1 and MC_2 during heating in vacuum and subsequent addition of water (0.1 mbar) at 130°C (Spectra and peak fits can be found in the supporting information)

Sample	**Process Step**	**Fraction O-Species [%]**						**Total oxygen content [%]**
		I 530.5	**II 531.2**	**III 531.9**	**IV 532.7**	**V 533.5**	**VI 534.2**	
MC_1	RT	0.4	1.5	1.4	3.0	4.0	0.8	11.1
	80°C	0.4	1.3	1.2	2.2	3.8	0.9	10.3
	130°C	0.4	1.4	1.2	1.9	3.7	0.9	9.4
	130°C_{vapor}	0.2	1.3	1.1	1.3	4.1	0.6	8.5
MC_2	RT	0.4	1.8	1.6	3.4	4.4	0.5	12.1
	80°C	0.4	1.7	1.4	2.6	4.3	0.5	10.9
	130°C	0.5	1.5	1.1	2.0	4.1	0.6	9.8
	130°C_{vapor}	0.2	1.4	1.1	1.3	4.1	0.2	8.3

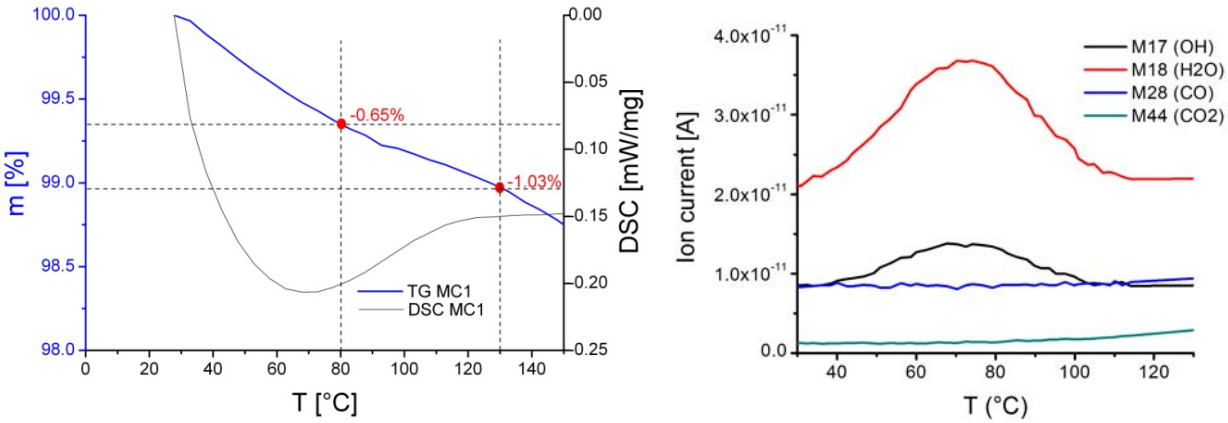

Figure 5: TG-MS experiment of MC_1. Left: mass loss over temperature treatment, Right: MS-signal for CO, CO_2, OH and H_2O.

Despite the similarity in the evolution of the O1s spectra, differences can be observed comparing the C1s spectra of the two samples (Figure 6). In case of MC_1 the carbon structure of the material remains almost unchanged during heating in vacuum. In contrary, an increase in amorphous surface carbon (284.7 eV) can be determined for MC_2. Generally the formation of amorphous surface carbon can be explained by the removal of oxygen functional groups while less ordered amorphous structures are retained. However, since the O1s spectra of both samples show similar losses in oxygen functional groups, this idea does not provide a satisfying explanation of the observations in the C1s spectra. For this reason, we would like to refer to the initial differences of the C1s spectra as discussed for the ex-situ XPS measurements. The effect of possible esterification reactions during the pretreatment in 2-butanol could be partially reversed by the water evolved during heating. Thus, hydrolysis and re-formation of hydrogen bonds can lead to structural changes. The increase in wettability and intercalation of water can result in the exfoliation of the structure. It is possible that less stable amorphous components can be partially transported towards the surface by the water evolved, resulting in the detection of higher amounts of amorphous surface carbon.

Since for none of the oxygen related features at higher binding energies of the C1s spectra a pronounced loss was observed, the strong changes in O1s spectra for both samples are unlikely to be related to the significant cleavage of C-O-bonds. More plausible for the explanation of the changes in the feature at 532.7 eV is the removal of structural water, e. g. from water incorporation of the pores or the solvation of oxygen functional groups.

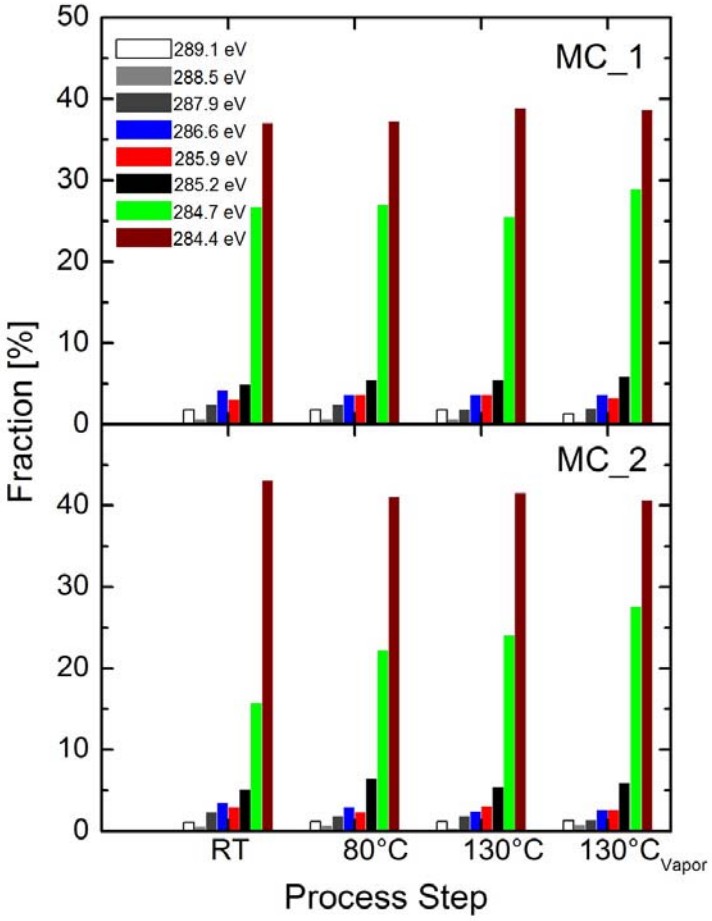

Figure 6: Evolution of C1s components during heating in vacuum and subsequent addition of water (0.1 mbar) at 130°C (Spectra and peak fits can be found in the supporting information).

3.3 Behavior during heating in water atmosphere

Compared to the experiments in vacuum, there are significant differences in the behavior of the two samples MC_1 and MC_2 while heating under water vapor of 0.1 mbar. The presence of water induces the additional reactivity of hydrolysis to the sequence of chemical events upon thermal treatment. The latter commonly leads to condensation reactions. Whereas the overall oxygen content for MC_2 does not change significantly under the heat treatment in vapor (even shows a tendency to rise up to 80°C), the total O-content for MC_1 decreases from 11.1% to 9.9% (Table 5).

Table 5: Quantification of oxygen species for MC_1 and MC_2 during heating in 0.1 mbar water vapor (Spectra and peak fits can be found in the supporting information)

Sample	Process Step	Fraction O-Species [%]						Total oxygen content [%]
		I 530.5	II 531.2	III 531.9	IV 532.7	V 533.5	VI 534.2	
MC_1	RT_{vapor}	0.1	1.6	1.4	3.3	4.6	0.9	11.8
	$80°C_{vapor}$	0.2	1.0	1.3	1.9	3.2	1.1	8.7
	$130°C_{vapor}$	0.5	1.6	1.3	1.7	3.4	1.5	9.9
MC_2	RT_{vapor}	0.2	1.1	1.4	2.4	3.7	0.3	9.2
	$80°C_{vapor}$	0.1	1.1	1.4	2.3	4.1	0.8	9.8
	$130°C_{vapor}$	0.1	1.1	1.4	1.6	4.0	1.4	9.5

The signal at 533.5 eV, which was stable for both samples during the heat treatment in vacuum, decreases for MC_1 while heating in water atmosphere. This indicates that parts of the ether or ester groups of MC_1 are sensitive against hydrolysis. In case of MC_2, the functional groups recorded at 533.5 eV are more stable against hydrolysis. On reason can be lower penetration of water into the structure due to the more hydrophobic surface.

Hydrolysis reactions have an oxygen introducing effect. Thus the small changes in the overall oxygen content for MC_2 could be the result of two simultaneous processes: Firstly, the loss of oxygen species (water removal) due to the increasing temperature and secondly the partial introduction of oxygen functional groups by possible hydrolysis reactions. Figure 7 summarizes potential hydrolysis reactions for the prior suggested surface functional groups of the materials. As a result of the hydrolysis, the surface solvation is enhanced, due to the increase in functional groups that are capable of hydrogen bond formation. Solvation or the incorporation of water molecules could be one explanation of restructuring forces as discussed before.

As a common trend of the O1s spectra, both samples, MC_1 and MC_2, exhibit a decrease of the peak located at 532.7 eV, also observed under vacuum. At the same time, the feature at the binding energy of 534.2 eV increases in intensity. The opposite trend of development of both

peaks supports the idea of two simultaneous processes. The correlation of the peak at 534.2 eV to OH-species in carboxyl functional groups corresponds to an often reported assignment in the literature [17, 20, 26, 27, 33]. In addition, carboxyl groups are preferentially formed in most hydrolysis reactions (Figure 7). Based on the reaction conditions applied, i. e. mild temperatures and vapor atmosphere, the decrease in the peak at 532.7 eV is most likely related to adsorbed water from pore incorporation or material solvation.

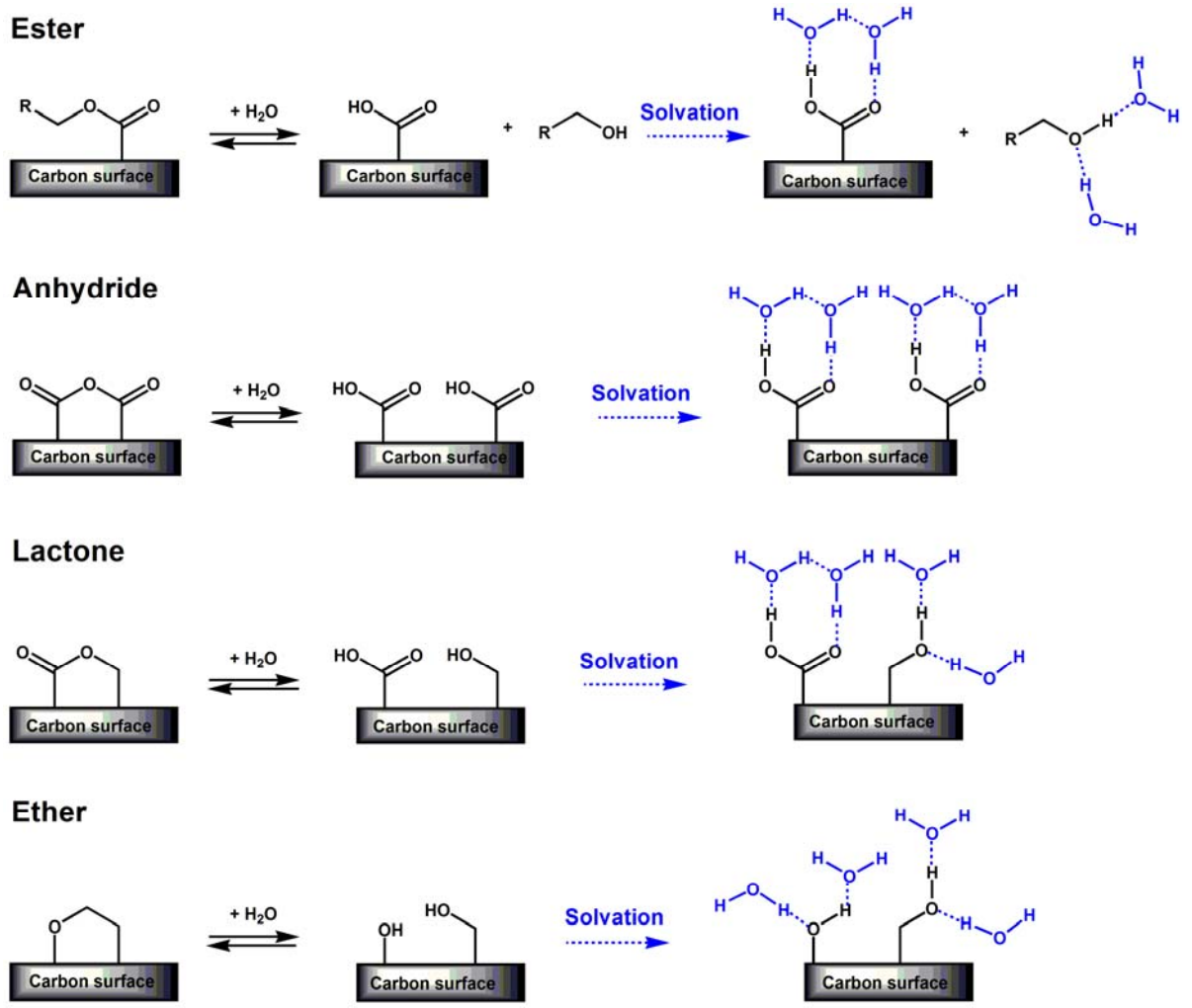

Figure 7: Reactivity of different oxygen functional groups towards water [36] and consequential changes in the solvation chemistry.

The C1s spectra for the experiments in water atmosphere reveal a stronger contribution of amorphous carbon for both samples (Figure 8), in comparison to the water-free experiments. In case of MC_1 a dramatic increase of the amorphous carbon can be followed during heating in vapor. Similar to the observations from the O1s spectra, MC_1 seems to be less stable against water.

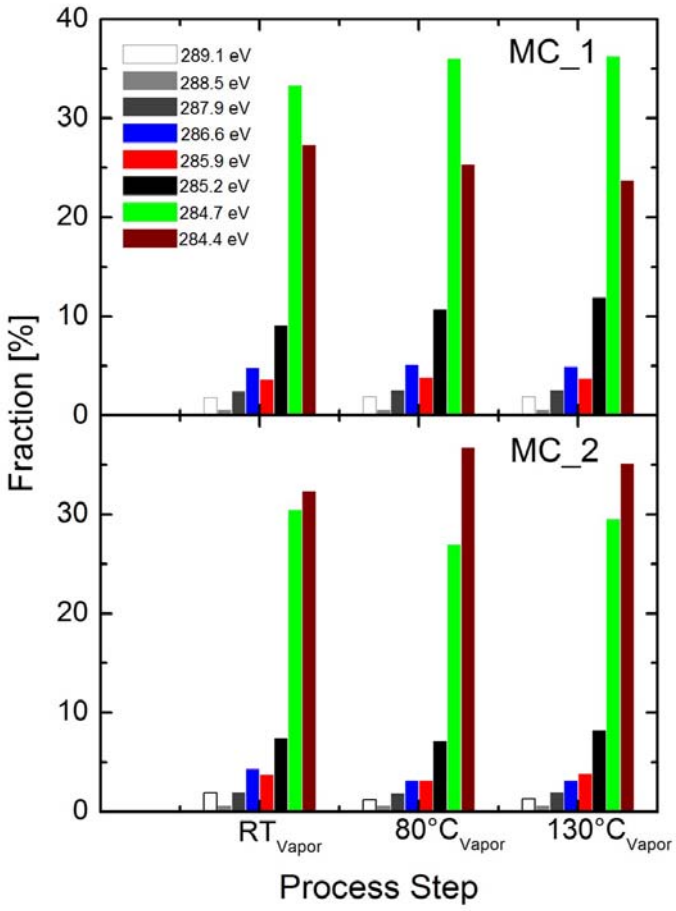

Figure 8: Evolution of C1s components during heating under water vapor of 0.1 mbar (Spectra and peak fits can be found in the supporting information).

4. Conclusions

The present study revealed two possible reasons for the deactivation of the carbon catalyst after the pretreatment in alcoholic solvent: 1. The lower content of oxygen species detected at 534.2 eV which can be assigned to carboxylic acid functional groups [17, 20, 26, 27, 33]. 2. The deactivation by esterification of acid functional groups, as indirectly evidenced by lower reactivity against water and the more hydrophobic surface of MC_2.

Apart from the results relevant for the catalytic application, the experiments provide crucial information on general properties of oxygen functionalized carbon in contact of water. Despite the similarities in the oxygen content and the evolution of the O1s peak during heating in vacuum, the addition of water and adjacent heat treatments revealed significant differences in the behavior of the two samples. Hence, carbon materials are not necessarily inert towards water if they carry oxygen functional groups. Carbon, if not graphitic, exhibits a dynamic behavior under the influence of water. Since the in-situ XPS experiment have been performed in only 0.1 mbar vapor pressure and mild temperatures of maximal 130°C, more drastic changes in the structure of carbon materials can be expected under “real” hydrothermal or electrochemical conditions. Several conclusions of the behavior of carbon materials under the influence of aqueous media, e. g. for electrode materials, can be reconsidered based on the finding of the presented XPS experiments.

Acknowledgements

The authors thank Gisela Lorenz for the BET measurements and Andrey Tarasov for TG-MS.

References

[1] Probstle H, Schmitt C, Fricke J. Button cell supercapacitors with monolithic carbon aerogels. J Power Sources. 2002;105(2):189-94.

[2] Wencui L, Reichenauer G, Fricke J. Carbon aerogels derived from cresol-resorcinol-formaldehyde for supercapacitors. Carbon. 2002;40(15):2955-29592959.

[3] Moreno-Castilla C, Maldonado-Hodar FJ, Rivera-Utrilla J, Rodriguez-Castellon E. Group 6 metal oxide-carbon aerogels. Their synthesis, characterization and catalytic activity in the skeletal isomerization of 1-butene. Applied Catalysis a-General. 1999;183(2):345-56.

[4] Zhao XC, Wang AQ, Yan JW, Sun GQ, Sun LX, Zhang T. Synthesis and Electrochemical Performance of Heteroatom-Incorporated Ordered Mesoporous Carbons. Chem Mat. 2010;22(19):5463-73.

[5] Hanzawa Y, Hatori H, Yoshizawa N, Yamada Y. Structural changes in carbon aerogels with high temperature treatment. Carbon. 2002;40(4):575-81.

[6] Samant PV, Goncalves F, Freitas MMA, Pereira MFR, Figueiredo JL. Surface activation of a polymer based carbon. Carbon. 2004;42(7):1321-5.

[7] Pekala RW. Organic aerogels from the polycondensation of resorcinol with formaldehyde. Journal of Materials Science. 1989;24(9):3221-7.

[8] Ruben GC, Pekala RW, Tillotson TM, Hrubesh LW. Imaging aerogels at the molecular level. Journal of Materials Science. 1992;27(16):4341-9.

[9] Christiansen AW. Resorcinol-formaldehyde reactions in dilute solution observed by carbon-13 NMR spectroscopy. J Appl Polym Sci. 2000;75(14):1760-8.

[10] Bluhm H, Haevecker M, Knop-Gericke A, Kiskinova M, Schloegl R, Salmeron M. In situ x-ray photoelectron spectroscopy studies of gas-solid interfaces at near-ambient conditions. Mrs Bulletin. 2007;32(12):1022-30.

[11] Knop-Gericke A, Kleimenov E, Haevecker M, Blume R, Teschner D, Zafeiratos S, et al. X-Ray Photoelectron Spectroscopy for Investigation of Heterogeneous Catalytic Processes. Advances in Catalysis, Vol 52. 2009;52:213-72.

[12] Salmeron M, Schlogl R. Ambient pressure photoelectron spectroscopy: A new tool for surface science and nanotechnology. Surface Science Reports. 2008;63(4):169-99.

[13] Vass EM, Haevecker M, Zafeiratos S, Teschner D, Knop-Gericke A, Schloegl R. The role of carbon species in heterogeneous catalytic processes: an in situ soft x-ray photoelectron spectroscopy study. Journal of Physics-Condensed Matter. 2008;20(18).

[14] Ketteler G, Ashby P, Mun BS, Ratera I, Bluhm H, Kasemo B, et al. In situ photoelectron spectroscopy study of water adsorption on model biomaterial surfaces. Journal of Physics-Condensed Matter. 2008;20(18).

[15] Kundu S, Wang YM, Xia W, Muhler M. Thermal Stability and Reducibility of Oxygen-Containing Functional Groups on Multiwalled Carbon Nanotube Surfaces: A Quantitative High-Resolution XPS and TPD/TPR Study. J Phys Chem C. 2008;112(43):16869-78.

[16] Schlogl R, Loose G, Wesemann M. On the mechanism of the oxidation of graphite by molecular oxygen. Solid State Ion. 1990;43:183-92.

[17] Biniak S, Szymanski G, Siedlewski J, Swiatkowski A. The characterization of activated carbons with oxygen and nitrogen surface groups. Carbon. 1997;35(12):1799-810.

[18] Martinez MT, Callejas MA, Benito AM, Cochet M, Seeger T, Anson A, et al. Sensitivity of single wall carbon nanotubes to oxidative processing: structural modification, intercalation and functionalisation. Carbon. 2003;41(12):2247-56.

[19] Desimoni E, Casella GI, Morone A, Salvi AM. XPS determination of oxygen-containing functional groups on carbon fiber surfaces and cleaning of these surfaces. Surface and Interface Analysis. 1990;15(10):627-34.

[20] Darmstadt H, Roy C, Kaliaguine S. ESCA characterization of commercial carbon blacks and of carbon blacks from vacuum pyrolysis of used tires. Carbon. 1994;32(8):1399-406.

[21] Clark DT, Cromarty BJ, Dilks A. ESCA applied to polymers. 24. Theoretical investigation of molecular core binding and relaxation energies in a series of oxygen-containing organic molecules of interest in the study of surface oxidation of polymers. J Polym Sci Pol Chem. 1978;16(12):3173-84.

[22] Clark DT, Dilks A. ESCA applied to polymers. 23. RF glow discharge modification of polymers in pure oxygen and helium oxygen mixtures. J Polym Sci Pol Chem. 1979;17(4):957-76.

[23] Rosenthal D, Ruta M, Schloegl R, Kiwi-Minsker L. Combined XPS and TPD study of oxygen-functionalized carbon nanofibers grown on sintered metal fibers. Carbon. 2010;48(6):1835-43.

[24] Lopez GP, Castner DG, Ratner BD. XPS O1s binding energies for polymers containing hydroxyl, ether, ketone and ester groups. Surface and Interface Analysis. 1991;17(5):267-72.

[25] Figueiredo JL, Pereira MFR, Freitas MMA, Orfao JJM. Modification of the surface chemistry of activated carbons. Carbon. 1999;37(9):1379-89.

[26] Figueiredo JL, Pereira MFR. The role of surface chemistry in catalysis with carbons. Catal Today. 2010;150(1-2):2-7.

[27] Schuster ME, Havecker M, Arrigo R, Blume R, Knauer M, Ivleva NP, et al. Surface Sensitive Study To Determine the Reactivity of Soot with the Focus on the European Emission Standards IV and VI. J Phys Chem A. 2011;115(12):2568-80.

[28] Frank B, Rinaldi A, Blume R, Schlogl R, Su DS. Oxidation Stability of Multiwalled Carbon Nanotubes for Catalytic Applications. Chem Mat. 2010;22(15):4462-70.

[29] Stein A, Wang Z, Fierke MA. Functionalization of Porous Carbon Materials with Designed Pore Architecture. Advanced Materials. 2009;21(3):265-93.

[30] Akhter MS, Chughtai AR, Smith DM. The structure of hexane soot I Spectroscopic studies. Appl Spectrosc. 1985;39(1):143-53.

[31] Smith DM, Chughtai AR. The surface structure and reactivity of black carbon. Colloids and Surfaces a-Physicochemical and Engineering Aspects. 1995;105(1):47-77.

[32] Desimoni E, Casella GI, Cataldi TRI, Salvi AM, Rotunno T, Dicroce E. Remarks on the surface characterization of carbon fibers. Surface and Interface Analysis. 1992;18(8):623-30.

[33] Zielke U, Huttinger KJ, Hoffman WP. Surface-oxidized carbon fibers .1. Surface structure and chemistry. Carbon. 1996;34(8):983-98.

[34] Schuster ME. Structure and Reactivity of Diesel Soot Particles from Advanced Motor Technologies. Technische Universität Berlin, 2011.

[35] Ruben GC, Pekala RW, Tillotson TM, Hrubesh LW. Imaging aerogels at the molecular level. Journal of Materials Science. 1992;27(16):4341-9.

[36] Breitmaier E, Jung G. Organische Chemie - Grundlagen, Stoffklassen, Reaktionen, Konzepte, Molekülstruktur. 5 ed. Stuttgart, New York: Georg Thieme Verlag; 2005.

Supplementary Information

SI 1. Nitrogen adsorption measurements

Table 6: BET isotherms of mesoporous carbon samples investigated by XPS

Sample	SN	BET isotherm	BJH poresize distribution
MC_0	10921	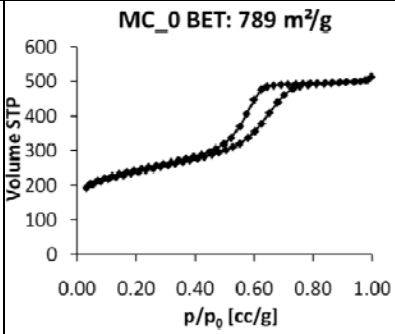	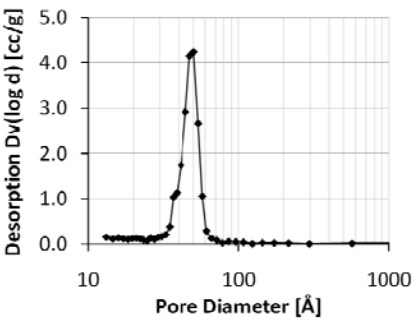
TDP0.2	11108	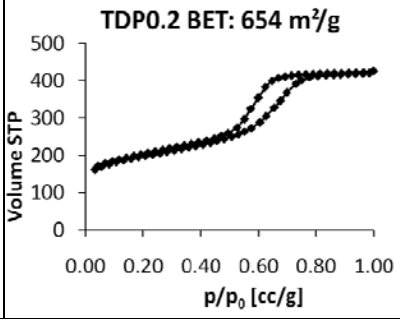	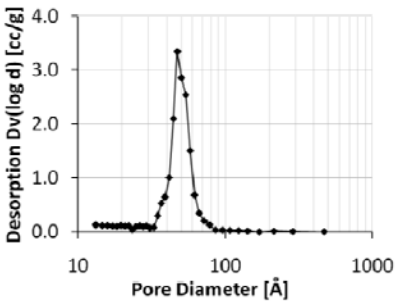
MC_1	11466	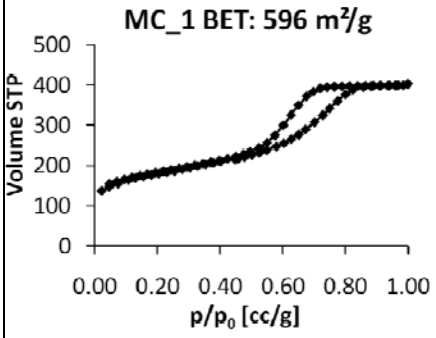	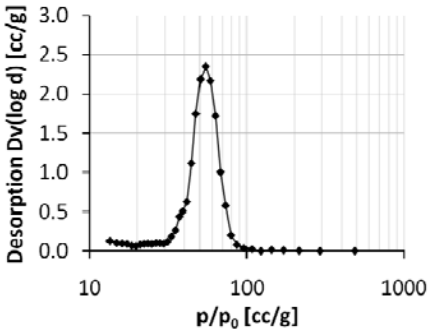
MC_2	11690	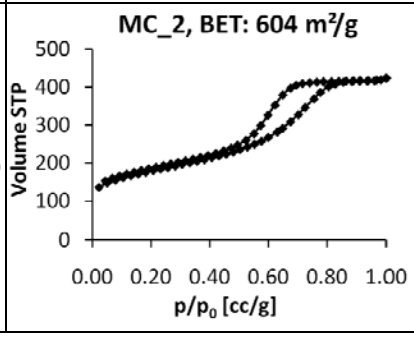	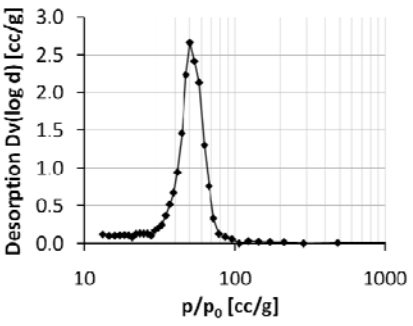

SI 2. Cl impurities and their evolution during heat and vapor treatment

Table 7: Quantification of Cl species of MC_1 and MC_2 during in-situ XPS

Experiment		Process step	Total Cl content [%]
Heating in vacuum and subsequent addition of 0.1 mbar vapor	MC_1	RT	0.4
		80°C	0.2
		130°C	0.2
		$130°C_{vapor}$	0.1
	MC_2	RT	0.2
		80°C	0.1
		130°C	0.1
		$130°C_{vapor}$	0.1
Heating in 0.1 mbar vapor pressure	MC_1	RT_{vapor}	0.3
		$80°C_{vapor}$	0.3
		$130°C_{vapor}$	0.2
	MC_2	RT_{vapor}	0.2
		$80°C_{vapor}$	0.2
		$130°C_{vapor}$	0.3

The acidic pH during the oxidation treatment in hydrogen peroxide is achieved by the addition of hydrochloric acid to the reaction mixture. As observed in the survey spectra, part of the hydrochloric acid reacted with the carbon material and formed chloro-functionalized surface species on the material. In order to give a complete comparison of the two samples MC_1 and MC_2 the Cl2p peaks have been examined in detail. The main feature of the Cl2p is located at ~200.4 eV. This can be related to chlorinated polymers like polyethylene or chlorinated benzene-like molecules [Moulder J, Stickle W, Sobol P. Handbook of X Ray Photoelectron Spectroscopy; 1992]. Sample MC_2 exhibits a smaller amount of Cl than sample MC_1 at room temperature (Table 7) and only MC_1 shows a decrease of the Cl signal with increasing T under vacuum conditions. This effect proceeds also under water exposure at 130°C, where the intensity of MC_1 reaches values comparable to the average Cl signal of MC_2. The addition of vapor during

the heat treatment seems to stabilize the Cl-functional groups in both samples. Minor differences were detected both for the different samples MC_1 and MC_2, as well as for the different temperature steps.

Although the total amount of chlorine functional groups is with < 0.5% small in comparison to 12% oxygen content, an effect on the catalytic performance of the two materials cannot be excluded.

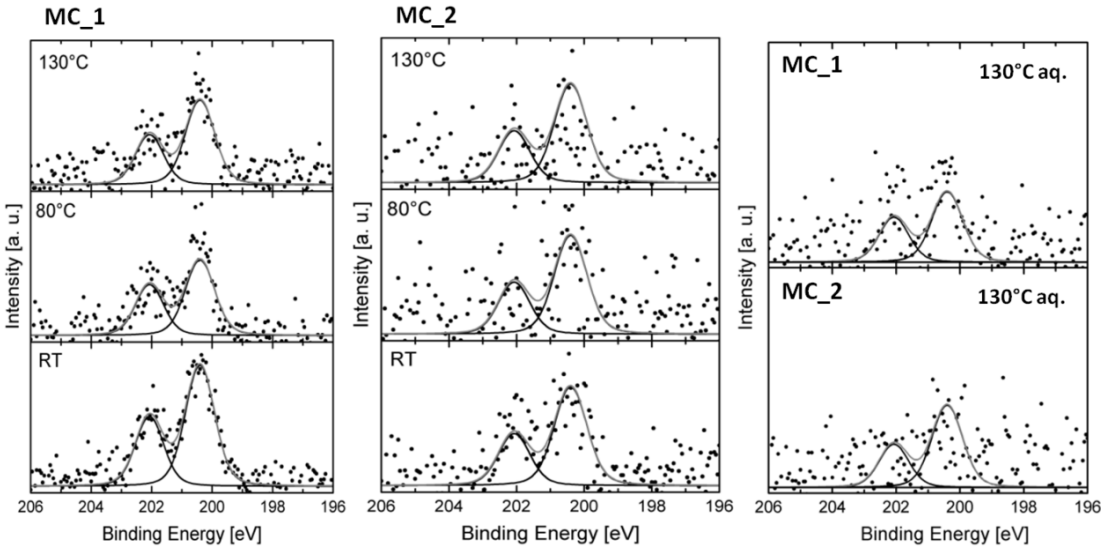

Figure 9: Cl 2p spectra for MC_1 and MC_2 during heating in vacuum

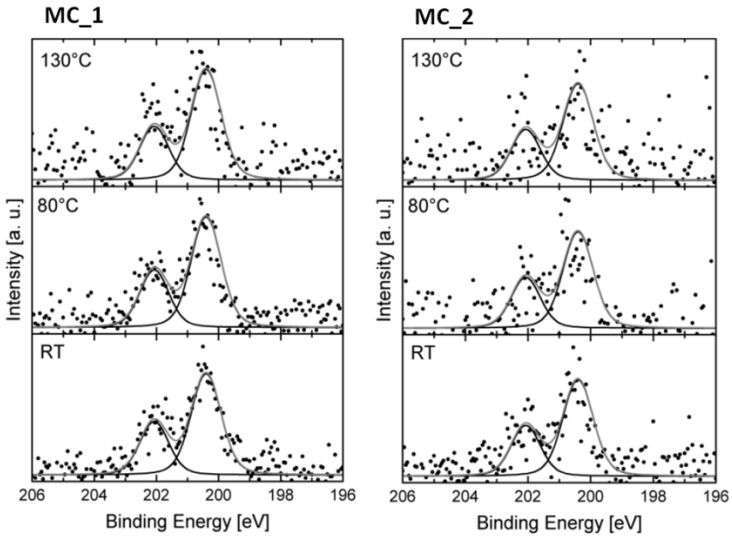

Figure 10: Cl 2p spectra for MC_1 and MC_2 during heating in vapor

SI 3. Additional information on evaluation of C1s and O1s signals

Table 8: Quantification of oxygen species of MC_0, MC_1 and MC_2 by ex-situ XPS [%]

Sample	530.5 eV	531.2 eV	531.9 eV	532.7 eV	533.5 eV	534.2 eV	Total oxygen content
MC_0	0.3	0.5	0.8	1.6	1.9	0.2	5.3
MC_1	0.4	1.5	1.4	3.0	4.0	0.8	11.1
MC_2	0.4	1.8	1.6	3.4	4.4	0.5	12.1

Table 9: Quantification of carbon species in the C1s pectra of MC_0, MC_1 and MC_2 obtained by ex-situ XPS [%]

Sample	284.4 eV	284.7 eV	285.2 eV	285.9 eV	286.6 eV	287.9 eV	288.5 eV	289.1 eV	Total carbon content
MC_0	40.0	27.7	4.7	2.4	2.9	1.8	5.9	1.2	94.8
MC_1	37.0	26.7	4.9	3.0	4.0	2.4	0.6	1.8	88.6
MC_2	43.0	15.7	5.1	2.9	3.4	2.3	0.5	1.1	87.7

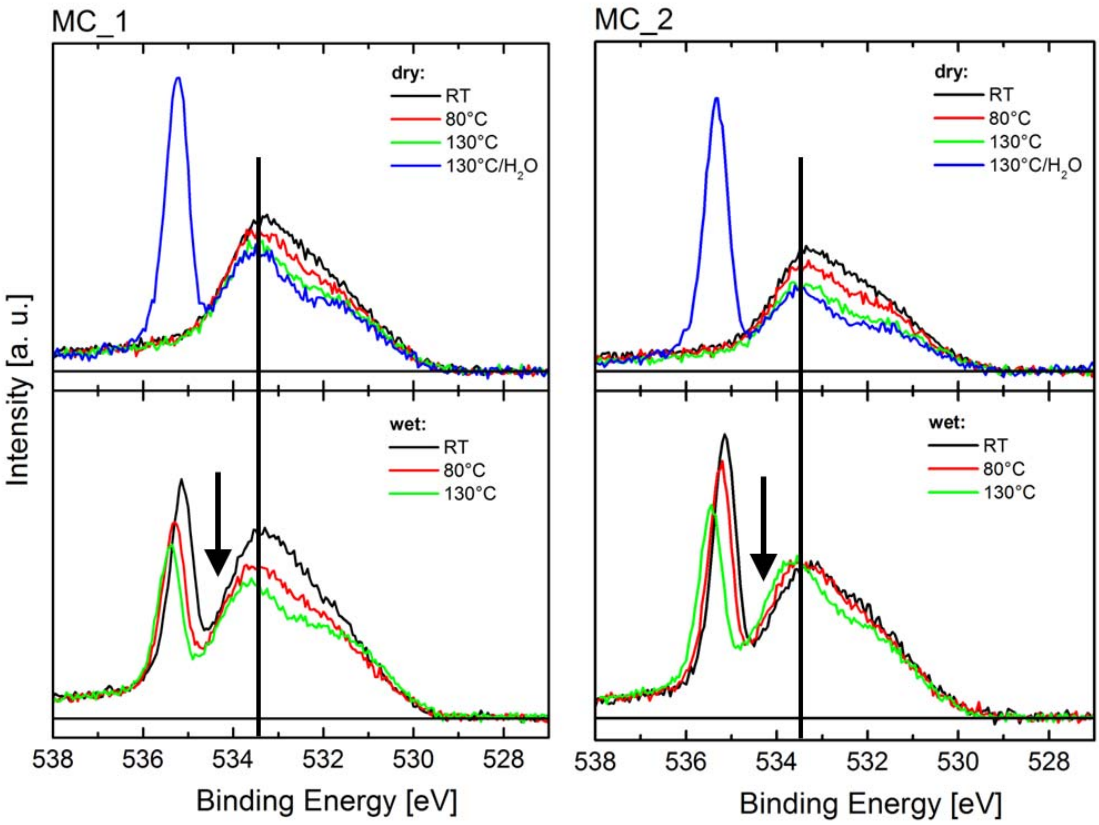

Figure 11: Insitu XPS spectra of sample MC1 (left) and MC2 (right). The line in the figure corresponds to the main intense 533.4 eV peak. The arrow points to a new feature developing while water exposure.

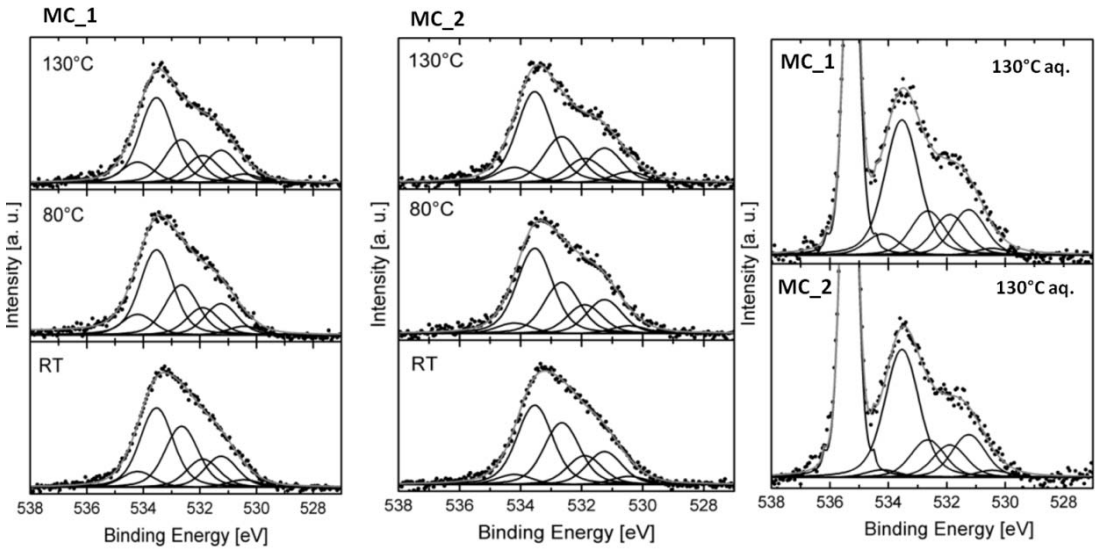

Figure 12: Fits for O1s spectra of MC_1 and MC_2 during heating in vacuum

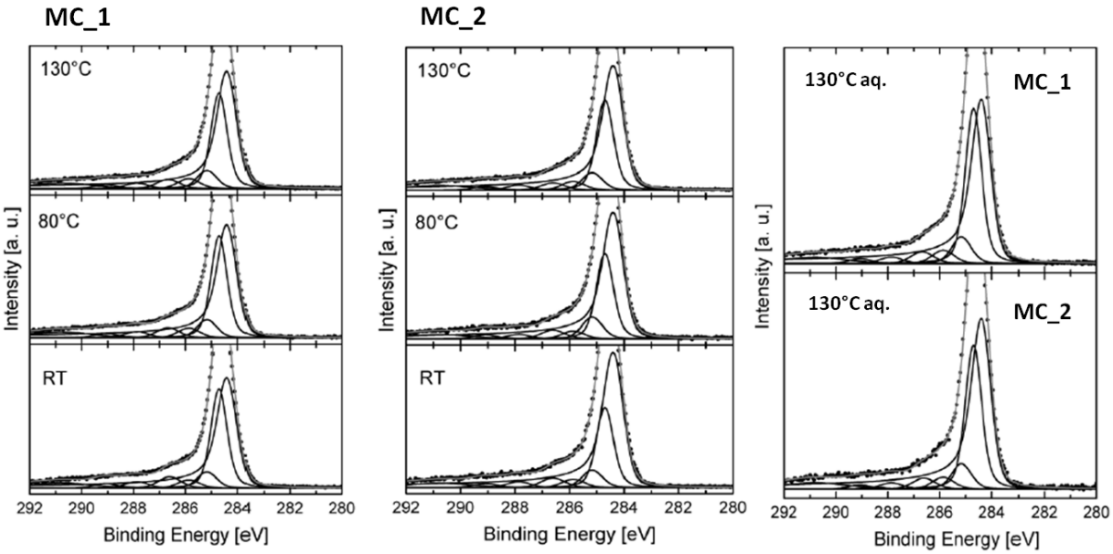

Figure 13: Fits for C1s spectra of MC_1 and MC_2 during heating in vacuum

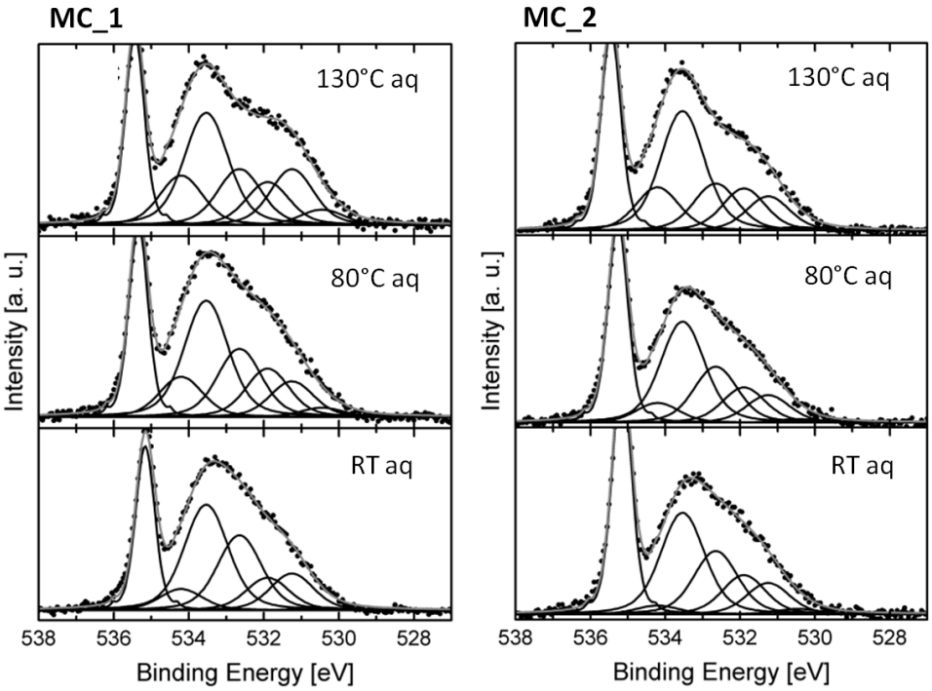

Figure 14: Fits for O1s spectra of MC_1 and MC_2 during heating in 0.1 mbar vapor

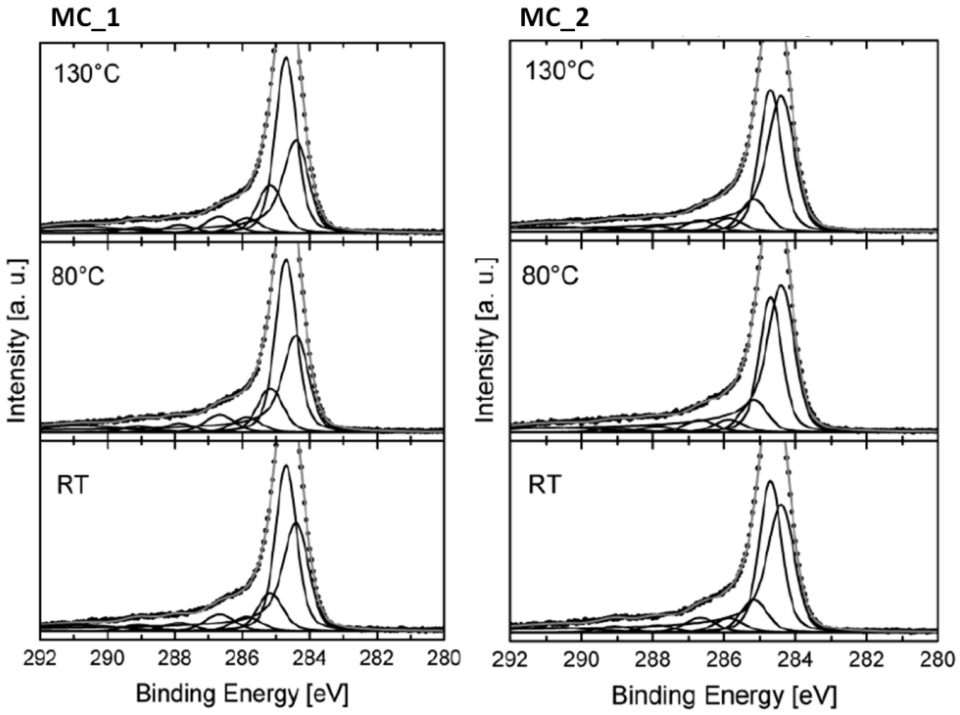

Figure 15: Fits for C1s spectra of MC_1 and MC_2 during heating in 0.1 mbar vapor